

# LHC and ILC probes of hidden-sector gauge bosons

Jason Kumar<sup>a</sup> and James D. Wells<sup>b</sup>

<sup>a</sup> Physics Department, Texas A&M University, College Station, TX 77843

<sup>b</sup> Michigan Center for Theoretical Physics (MCTP)

Department of Physics, University of Michigan, Ann Arbor, MI 48109

Intersecting D-brane theories motivate the existence of exotic  $U(1)$  gauge bosons that only interact with the Standard Model through kinetic mixing with hypercharge. We analyze an effective field theory description of this effect and describe the implications of these exotic gauge bosons on precision electroweak, LHC and ILC observables.

*Exotic abelian symmetries.* There are many reasons to suspect that nature contains more abelian factors than just hypercharge of the Standard Model (SM). Traditionally, these abelian groups were thought to arise as subgroups of larger unification groups, such as  $SO(10) \rightarrow G_{SM} \times U(1)$  or  $E_6 \rightarrow G_{SM} \times U(1)^2$ . This motivation for extra  $U(1)$  gauge groups led to studies of exotic  $Z'$  bosons that coupled at tree-level to the SM particles [1, 2, 3].

In this letter, we wish to emphasize the brane world motivation for extra  $U(1)$  factors and study their consequences for phenomenology within an effective theory framework. To begin with we note a basic fact: a stack of  $N$  coincident branes gives rise to the gauge group  $U(N)$ , which is decomposed into  $SU(N) \times U(1)$ . There are typically many stacks of coincident branes in a complete, self-consistent string theory of particle physics. Unless the branes are at special points in the extra-dimensional space, they will produce at least one abelian factor for every stack. Of these, a few combinations are anomaly free and massless (see, e.g., [4, 5, 6, 7, 8, 9]).

Brane-world  $U(1)$ 's are special (compared to GUT  $U(1)$ 's) because there is no generic expectation that SM particles will be charged under them. When a SM-like theory is constructed in brane-world scenarios, the SM particles generally arise as open strings connecting one SM brane stack to another. Exotic non-SM branes usually carry the extra  $U(1)$  factors.

*Effective theory description.* The framework described above gives rise to the possibility that an exotic  $U(1)_X$  gauge symmetry exists that survives down to the TeV scale, but has no direct couplings to SM particles. Our effective field theory description at a scale  $\Lambda \gg m_Z$  has Standard Model (SM) gauge group and an additional  $U(1)_X$ . There are three sectors of matter particles

- *Visible Sector:* Particles charged under the SM but not under  $U(1)_X$ . The SM particles (quarks, leptons, Higgs, neutrinos) comprise this sector.
- *Hidden Sector:* Particles charged under  $U(1)_X$ , but singlets under the SM gauge groups.
- *Hybrid Sector:* Particles charged under both the SM and  $U(1)_X$  gauge groups, which we call *kinetic messengers* since they can induce kinetic mixing between  $U(1)_X$  and SM hypercharge.

From the D-brane point of view, the hybrid sector of kinetic messengers come from open strings connecting a SM brane stack to a hidden sector brane stack.

There are one-loop quantum corrections that mix the kinetic terms of  $U(1)_Y$  and  $U(1)_X$  [10, 11, 12, 13, 14, 15]. We are then left with an effective Lagrangian at scale  $\mu$  for the kinetic terms of the form:

$$L_K = -\frac{1}{4}\hat{B}_{\mu\nu}\hat{B}^{\mu\nu} - \frac{1}{4}\hat{X}_{\mu\nu}\hat{X}^{\mu\nu} + \frac{\chi}{2}\hat{B}_{\mu\nu}\hat{X}^{\mu\nu} \quad (1)$$

where  $\chi$  is given by

$$\chi = \frac{\hat{g}_Y \hat{g}_X}{16\pi^2} \sum_i Q_X^i Q_Y^i \log\left(\frac{m_i^2}{\mu^2}\right) \quad (2)$$

and the sum  $i$  is over all kinetic messenger states.

We cannot say what value of  $\chi$  is typical in the many possible brane-world models of particle physics. Although the above equation is a one-loop expression, and perhaps expected to be small, the multiplicity of states could be large enough to compensate for the one-loop suppression. In a different context, the issue of kinetic mixing among exotic  $U(1)$ 's was investigated by Dienes, Kolda and March-Russell [10], and it was estimated that  $10^{-3} < \chi < 10^{-2}$ ; however, this estimate may not be applicable for other approaches to model building.

One can choose a field redefinition  $\hat{X}_\mu, \hat{Y}_\mu \rightarrow X_\mu, Y_\mu$  that makes the kinetic terms of eq. 1 diagonal and canonical. The most convenient choice of diagonalization is one in which the couplings to  $Y$  are independent of  $Q_X$ :

$$\begin{pmatrix} X_\mu \\ Y_\mu \end{pmatrix} = \begin{pmatrix} \sqrt{1-\chi^2} & 0 \\ -\chi & 1 \end{pmatrix} \begin{pmatrix} \hat{X}_\mu \\ \hat{Y}_\mu \end{pmatrix}. \quad (3)$$

The covariant derivative is now:

$$D_\mu \rightarrow \partial_\mu + i(g_X Q_X + \eta g_Y Q_Y)X_\mu + i g_Y Q_Y Y_\mu, \quad (4)$$

where

$$g_Y = \hat{g}_Y, \quad g_X \equiv \frac{\hat{g}_X}{\sqrt{1-\chi^2}}, \quad \eta \equiv \frac{\chi}{\sqrt{1-\chi^2}}. \quad (5)$$

(Note,  $\eta \simeq \chi$  for small  $\chi$ .) We are considering the case where  $U(1)_X$  is broken due to the veving of a hidden sector Higgs field  $\Phi_X$  with  $Q_X \neq 0$  and  $Q_Y = 0$ .  $X_\mu$  then

gets a mass  $m_X^2 \sim g_X^2 \langle \Phi_X \rangle^2$ , while  $Y$  stays massless. It is somewhat natural that  $m_X$  is of order weak scale or TeV scale, especially if the vev is controlled by supersymmetry breaking. Note, the covariant derivative couples matter to  $Y$  in the same way as to  $\hat{Y}$ . Thus, we can identify  $Y$  as the hypercharge gauge boson.

SM particles couple to  $X^\mu$  with strength  $\eta g_Y Q_Y$ , i.e. with couplings proportional to hypercharge. This is an important phenomenological implication that enables  $X_\mu$  to be probed by experiments involving SM particles. The  $X_\mu$  behaves as a resonance of the hypercharge gauge boson with somewhat smaller coupling; indeed, it may be confused with an extra-dimension hypercharge gauge boson.

The  $U(1)_X$  also couples to hidden sector fields at tree-level. However, we assume the  $U(1)_X$  we are studying is too light to decay into on-shell hidden sector particles. Since the mass of light hidden sector particles will be set by the gauge-symmetry breaking scale, this will likely be correct provided we study the hidden  $U(1)$  which is broken at the lowest scale. If this assumption is wrong, the collider signatures that rely on branching fractions of  $X$  boson decays into SM particles would have to be adjusted.

*Mass Eigenstates after Electroweak Symmetry Breaking.* When  $SU(2) \times U(1)_Y$  breaks to  $U(1)_{em}$ , the  $Z_\mu$  and  $X_\mu$  eigenvalues mix due to the small coupling of  $X_\mu$  to condensing Higgs boson(s) that carry hypercharge. The effects of this mixing are minimal for the phenomenology of the  $X_\mu$  boson at high-energy colliders, except for two effects. First, the  $Z$  boson mass will be suppressed compared to SM expectations by a factor of  $\delta$  in

$$m_Z^2 = \frac{m_W^2}{\cos^2 \theta_W} (1 - \delta), \quad \text{where } \delta \simeq \eta^2 \sin^2 \theta_W \frac{m_Z^2}{m_X^2}. \quad (6)$$

This shift has an effect on the precision electroweak observables, which is characterized by a shift in the Peskin-Takeuchi  $T$  parameter [16]:

$$\Delta T = \frac{1}{\alpha} \delta \simeq \eta^2 \left( \frac{489 \text{ GeV}}{m_X} \right)^2. \quad (7)$$

Experimental measurements of  $\Gamma_Z$ ,  $m_W$ ,  $\sin^2 \theta_W^{\text{eff}}$ , etc., put limits on  $\Delta T \lesssim 0.2$ . Thus, for kinetic mixing of  $\eta \sim \mathcal{O}(1)$ , we expect  $m_X \gtrsim 1 \text{ TeV}$  (if no other effects conspire to offset it), whereas for  $\eta \lesssim \mathcal{O}(0.1)$  we expect no meaningful bound from current precision electroweak.

The second consequence is that the mixing between the  $Z$  and  $X$  bosons can change the hypercharge coupling of  $X$  to SM particles. This is a subdominant effect for small  $m_Z^2/m_X^2$ , except it now allows the  $X$  boson mass eigenstate to decay into SM  $W$  bosons. After mixing, one finds that

$$\Gamma(X \rightarrow W^+ W^-) = \alpha \eta^2 m_X \left( \frac{m_Z}{m_X} \right)^4. \quad (8)$$

$\Gamma(W^+ W^-) \simeq 43 \text{ keV}$  when  $\eta = 0.1$  and  $m_X = 500 \text{ GeV}$ . This partial width is rather narrow, and for  $m_X > 200 \text{ GeV}$  it will be less than 2% of the width of  $X$  decaying into fermions, which is given by

$$\Gamma(X \rightarrow f \bar{f}) = \eta^2 \frac{N_c \alpha}{6 \cos^2 \theta_W} (Y_{f_L}^2 + Y_{f_R}^2) m_X. \quad (9)$$

Since we will generally consider somewhat larger masses, we may safely ignore  $WW$  decays.

*LHC Probes.* We are now in a position to examine the possible collider signatures of this scenario. The process most amenable to LHC analysis is on-resonance  $pp \rightarrow X \rightarrow \mu \bar{\mu}$ . The predominant backgrounds are  $pp \rightarrow \gamma^*/Z^* \rightarrow \mu \bar{\mu}$ .

For a hadron collider, observational bounds are somewhat model-independent. If we denote by  $N_X$  the number of signal events needed for a discovery signal, we find that the limit on the mass of a discoverable  $X$  is [2, 3]

$$m_X^{\text{lim}} \simeq \frac{\sqrt{s}}{A} \ln \left( \frac{L c_X C}{s N_X} \right), \quad (10)$$

where the details of the model are encoded in

$$c_X = \frac{4\pi^2}{3} \frac{\Gamma_X}{m_X} B(\mu \bar{\mu}) \left[ B(u \bar{u}) + \frac{1}{C_{ud}} B(d \bar{d}) \right].$$

For a  $pp(p\bar{p})$  collider,  $A = 32(20)$ ,  $C = 600(300)$ , and in the kinematical region of interest at LHC  $C_{ud} \sim 2$  and  $\sqrt{s} = 14 \text{ TeV}$ .  $L$  is the integrated luminosity. If  $m_X > m_X^{\text{lim}}$ ,  $X_\mu$  cannot be observed at the collider. The logarithmic dependence of the detection bound implies that this result is rather robust, somewhat insensitive to variations in detector efficiency, number of events needed for discovery, or small variations in luminosity.

Plugging in the appropriate branching fractions  $B(f \bar{f})$  yields  $c_X(X \rightarrow \mu \bar{\mu}) = 0.00456 \eta^2$  (for  $m_X < 2m_{top}$ , this will increase by  $< 15\%$ ). We will fix an integrated luminosity of  $100 \text{ fb}^{-1}$ , which is expected from LHC after a few years of high-luminosity running. We then find

$$m_X^{\text{lim}} \simeq 5.78 \text{ TeV} + (0.44 \text{ TeV}) \ln \eta^2 - (0.44 \text{ TeV}) \ln N_X$$

at  $100 \text{ fb}^{-1}$  integrated luminosity. Equivalently, we may write the lower limit on detectable kinetic mixing in terms of the the mass of the  $X$  and the number of signal events  $N_X$  as

$$\eta \geq \sqrt{N_X} e^{-6.61 + \frac{m_X}{0.88 \text{ TeV}}}$$

Using Pythia [17] to simulate the SM background in 50 GeV bins, we can then plot  $\frac{N_X}{\sqrt{N_{\text{bgd}}}}$  at LHC as a function of  $\eta$  and  $m_X$  (Fig.1). We see that realistic demands for a signal which can be distinguished from the background will require  $\eta > 0.03$ . Below the top threshold, the bounds on  $\eta$  may shift by  $< 8\%$ . Although this is unfortunately not a good probe when compared to naive

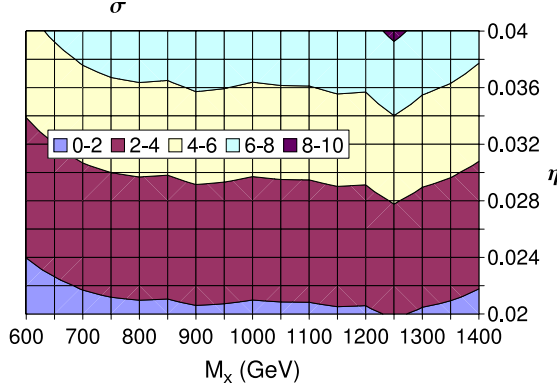


FIG. 1: LHC detection prospects for  $100 \text{ fb}^{-1}$  of integrated luminosity in the  $\eta$ - $M_X$  plane. The contours are of signal significance, which exceeds 5 only when  $\eta \gtrsim 0.03$ .

one-loop perturbative estimates, the multiplicity of kinetic messengers may enable  $\eta > 0.03$  and so should be studied with care at the LHC. A more sophisticated analysis, taking into account the precise nature of the backgrounds compared to the signal, might probe much smaller values of  $\eta$  at the LHC.

An analysis at Tevatron would be similar, but with different parameters (accounting for differences in specifications and for a  $p\bar{p}$  collider). We now have  $C_{ud} = 25$  and  $\sqrt{s} = 2 \text{ TeV}$ . Assuming an integrated luminosity of  $8 \text{ fb}^{-1}$ , the  $\eta$  sensitivity is

$$\eta_{\text{teva.}} \geq \sqrt{N_X} e^{-6.7 + \frac{m_X}{0.2 \text{ TeV}}}$$

For detection we would demand at least a  $5\sigma$  signal above background, or at least 10 events above background (whichever is larger). At  $m_X = 500 \text{ GeV}$  detection could only occur if  $\eta > 0.07$ . As  $m_X$  increases, the sensitivity limits on  $\eta$  degrade rapidly.

*ILC Prospects.* Given the challenge for LHC detection posed by small kinetic mixing, one might hope that ILC can do better. An  $e^+e^-$  collider will generally trade away  $\sqrt{s}$  for higher luminosity ( $\sim 500 \text{ fb}^{-1}$ ) and a cleaner signal. One does not produce an  $X$  on resonance, of course, unless its mass is less than the center of mass energy, which we assume here to be  $500 \text{ GeV}$ .

The basic process we are interested in is  $e^-e^+ \rightarrow \mu\bar{\mu}$  through  $\gamma^*/Z^*/X^*$ . The observable that provides perhaps the most useful signal in this case is the total cross-section [18] (the forward-backward asymmetry and left-right polarization do not appear to provide qualitative improvement). We may write the total cross-section as

$$\sigma_{\text{tot}}(f\bar{f}) = \frac{N_c}{48\pi s} \sum_{n,m} \frac{g_n^2 g_m^2 s^2 I_{m,n}^f}{(s - m_{V_n}^2)(s - m_{V_m}^2)^*} \quad (11)$$

where

$$I_{m,n}^f = (L_n^e L_m^{e*} + R_n^e R_m^{e*})(L_n^f L_m^{f*} + R_n^f R_m^{f*}) \quad (12)$$

and the coupling of the  $V_n$  boson to the fermions  $ff\bar{f}$  is given by  $ig_n\gamma^\mu(L_n^f P_L + R_n^f P_R)$ . If  $m_X > 500 \text{ GeV}$ , this

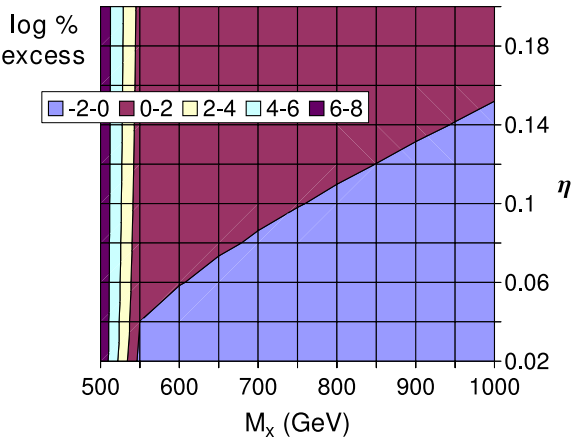


FIG. 2: Deviations of  $e^+e^- \rightarrow \mu\bar{\mu}$  at ILC at  $\sqrt{s} = 500 \text{ GeV}$  for  $500 \text{ fb}^{-1}$  integrated luminosity are represented in this plot as contours of the  $\log_{10}(\%)$  of the excess of events produced compared to SM expectations. The line along the interface of the blue and maroon regions represents a  $10^0 = 1\%$  (or  $\sim 5\sigma$ ) deviation.

observable will provide the dominant signal. Near the resonance, the signal is enhanced and we should replace:

$$\frac{1}{s - m_V^2} \Rightarrow \frac{(s - m_V^2) - i\Gamma_V \sqrt{s}}{(s - m_V^2)^2 + s\Gamma_V^2} \Rightarrow \frac{-i}{\Gamma_V m_V}. \quad (13)$$

Our strategy is to compare the inclusive cross-section for  $X$  production to the pure Standard Model background. Our criterion for a signal detection will be a 1% deviation from SM expectations (see Fig. 2). This corresponds to a  $\sim 5\sigma$  signal given the SM cross-section  $\sigma_{\text{tot}} = 447 \text{ fb}$  [19]. If  $m_X < 500 \text{ GeV}$ , then we should instead consider the hard-scattering process  $e^-e^+ \rightarrow \gamma X \rightarrow \gamma\gamma\bar{f}$ . The emission of a hard photon will allow us to scatter through a resonance of the  $X$ , enhancing the cross-section. This is a leading order calculation, as radiation of more photons would serve to enhance both the signal and backgrounds we calculate for the single photon case.

The differential cross-section of  $\gamma X$  production is

$$\frac{d\sigma}{dx} = \frac{\alpha(c_L^2 + c_R^2)[(s + m_X^2)^2 + (s - m_X^2)^2 x^2]}{4s^2(s - m_X^2)(1 - x^2)} \quad (14)$$

where  $x \equiv \cos\theta$  and  $i\gamma^\mu(c_L P_L + c_R P_R)$  are the couplings of the left and right handed electrons to  $X_\mu$ . We choose a standard  $|\cos\theta| < 0.95$  angular cut. The signal we analyze is  $X \rightarrow \mu\bar{\mu}$ , so we must multiply by the appropriate branching fraction,  $B(\mu\bar{\mu}) = 0.12$ . Plugging in the couplings we find

$$\sigma(\gamma X) = \eta^2 \frac{1.26 \times 10^{-3}}{s^2(s - m_X^2)} F(s, m_X, x_0), \quad \text{where}$$

$$F(s, m_X, x_0) = (s^2 + m_X^4) \tanh^{-1} x_0 - \frac{x_0}{2}(s - m_X^2)^2$$

and  $x_0 = |\cos\theta_{\min}| = 0.95$ . Comparing this signal to the Standard Model background  $e^+e^- \rightarrow \gamma\mu\bar{\mu}$  gives us signal

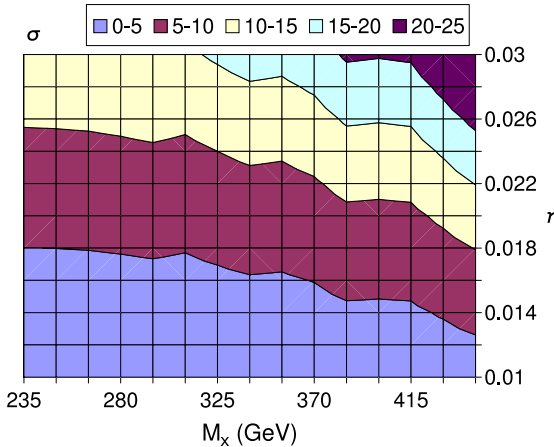


FIG. 3: Signal significance plot of  $e^+e^- \rightarrow \gamma X \rightarrow \gamma\mu\bar{\mu}$  at ILC  $\sqrt{s} = 500$  GeV with  $500 \text{ fb}^{-1}$  integrated luminosity. We assume that the  $m_{\mu\bar{\mu}}$  can be measured to within 2%.

significance at ILC for  $m_X < 500$  GeV as well (Fig. 3). We find that kinematically accessible  $X$  bosons at ILC-500 will be significantly better probed than at the LHC.

An analysis of LEP data proceeds in a similar manner. For  $m_X > \sqrt{s}$ , detection from LEP data is highly disfavored. For smaller  $m_X$ , however, resonance production (through hard photon emission) is allowed, which favors detection at LEP over hadron colliders such as LHC or the Tevatron. (We assume  $725 \text{ pb}^{-1}$  at  $\sqrt{s} = 206$  GeV.) But even here ILC provides better detection limits.

*Outlook.* We can summarize our results with a detection plot (Fig. 4). We see that for  $m_X \gtrsim 550$  GeV, LHC is more capable of detecting  $X_\mu$  in our scenario, while for  $m_X \lesssim 550$  GeV ILC-500 is more capable. Detection within the regime favored by a naive perturbative estimate of kinetic mixing ( $\eta \sim 10^{-3} - 10^{-2}$ ) appears difficult

at the LHC, but perhaps possible at the ILC as long as the gauge boson mass is at or below the center of mass energy of the ILC. Of course, a higher energy ILC (1 TeV and higher) will help the search for higher-mass  $X$  bosons. As we emphasized earlier, however, the amount of kinetic mixing can vary dramatically from one model to the next, depending on the multiplicity of the kinetic messengers, and thus all regions of phase space are candidates for discovery.

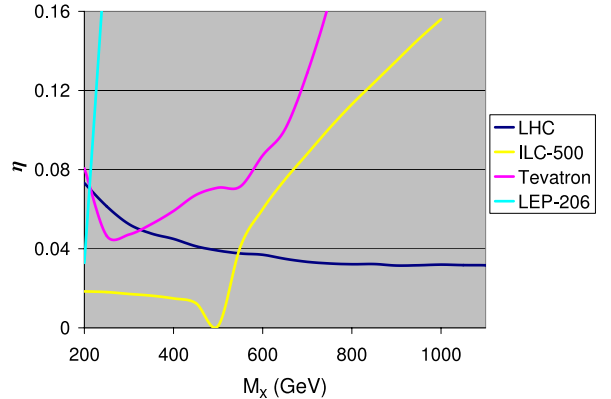


FIG. 4: Detection plot of estimated  $5\sigma$  confidence level of  $X$ -boson that kinetically mixes with hypercharge. Detection for Tevatron ( $8 \text{ fb}^{-1}$ ), LHC ( $100 \text{ fb}^{-1}$ ), LEP ( $\sqrt{s} = 206$  GeV and  $725 \text{ pb}^{-1}$ ), and ILC ( $\sqrt{s} = 500$  GeV and  $500 \text{ fb}^{-1}$ ) can occur at points above their respective lines.

*Acknowledgments.* We gratefully acknowledge B. Dutta, D. Morrissey, A. Rajaraman, G. Shiu and M. Toharia for helpful discussions. This work is supported by the Department of Energy, NSF Grant PHY-0314712 and the MCTP.

---

[1] M. Cvetic and P. Langacker, Phys. Rev. D **54**, 3570 (1996) [arXiv:hep-ph/9511378].  
[2] A. Leike, Phys. Lett. B **402**, 374 (1997) [arXiv:hep-ph/9703263].  
[3] J. Kang and P. Langacker, Phys. Rev. D **71**, 035014 (2005) [arXiv:hep-ph/0412190].  
[4] G. Aldazabal *et al.*, JHEP **0102**, 047 (2001) [arXiv:hep-ph/0011132].  
[5] R. Blumenhagen, M. Cvetic, P. Langacker and G. Shiu, arXiv:hep-th/0502005.  
[6] F. Marchesano and G. Shiu, JHEP **0411**, 041 (2004) [arXiv:hep-th/0409132].  
[7] J. Kumar and J. D. Wells, Phys. Rev. D **71**, 026009 (2005) [arXiv:hep-th/0409218]; JHEP **0509**, 067 (2005) [arXiv:hep-th/0506252]; arXiv:hep-th/0604203.  
[8] T. P. T. Dijkstra, L. R. Huiszoon and A. N. Schellekens, Nucl. Phys. B **710**, 3 (2005) [arXiv:hep-th/0411129].  
[9] F. Gmeiner *et al.*, JHEP **0601**, 004 (2006) [arXiv:hep-th/0510170].  
[10] K. R. Dienes, C. F. Kolda and J. March-Russell, Nucl. Phys. B **492**, 104 (1997) [arXiv:hep-ph/9610479].  
[11] S. P. Martin, Phys. Rev. D **54**, 2340 (1996) [arXiv:hep-ph/9602349].  
[12] F. del Aguila, M. Masip and M. Perez-Victoria, Nucl. Phys. B **456**, 531 (1995) [arXiv:hep-ph/9507455].  
[13] B. Holdom, Phys. Lett. B **166**, 196 (1986).  
[14] B. A. Dobrescu, Phys. Rev. Lett. **94**, 151802 (2005) [arXiv:hep-ph/0411004].  
[15] K. S. Babu, C. F. Kolda and J. March-Russell, Phys. Lett. B **408**, 261 (1997) [arXiv:hep-ph/9705414].  
[16] M. E. Peskin and T. Takeuchi, Phys. Rev. D **46**, 381 (1992).  
[17] T. Sjostrand, S. Mrenna and P. Skands, arXiv:hep-ph/0603175.  
[18] A. Leike, Z. Phys. C **62**, 265 (1994) [hep-ph/9311356].  
[19] A. Pukhov *et al.* (COMPHEP), arXiv:hep-ph/9908288.